Multiantenna Multisatellite Code and Carrier Tracking

Kaspar Giger, *Technische Universität München, Germany*
Christoph Günther, *Technische Universität München, and German Aerospace Center (DLR), Germany*

BIOGRAPHY

Kaspar Giger received the M.S. degree in electrical engineering and information technology from the Swiss Federal Institute of Technology (ETH), Zurich, Switzerland, in 2006. He is currently pursuing the Ph.D. degree at the Institute for Communications and Navigation, Technische Universität München, Munich, Germany, working on new signal tracking algorithms.

Christoph Günther studied theoretical physics at the Swiss Federal Institute of Technology (ETH), Zurich, Switzerland. He received his diploma in 1979 and completed his PhD in 1984. He worked on communication and information theory at Brown Boveri and Ascom Tech. From 1995, he led the development of mobile phones for GSM and later dual mode GSM/Satellite phones at Ascom. In 1999, he became head of the research department of Ericsson in Nuremberg. Since 2003, he is the director of the Institute of Communications and Navigation at the German Aerospace Center (DLR) and since December 2004, he additionally holds a Chair at the Technische Universität München, Munich, Germany. His research interests are in satellite navigation, communication, and signal processing.

ABSTRACT

In any radio navigation and radio communication system, receivers can be equipped with multiple antennas. By properly weighting and combining the different antenna signals after A/D conversion the wanted signals can be amplified and interfering signals suppressed (digital beamforming). But through the process of beamforming the information about the relative signal delays between the antenna elements is lost. In a multiantenna receiver the signals form multiple antennas are weighted and combined only after the phase discriminators (i.e. error detectors). This allows an estimation of the receiver platform attitude in parallel with the usual signal tracking. Due to the nonlinear relationship between the measurements and the attitude parametrization the problem of attitude estimation in the multiantenna tracking is non convex. A global convergence is achieved by combining a divergence detection together with a reinitialization scheme. Although the multiantenna tracking combines the measurements of multiple antennas in digital domain, it is inherently different from traditional digtial beamforming. The price the receiver has to pay for the attitude estimation is a reduced capability of amplifying and suppressing directive signals. But still a suppression of interfering signals is achieved. Simulation results indicate a fast convergence of the loop in parallel with a robust tracking lock. It can be concluded that multiantenna tracking is a valuable tool for jointly estimating the receiver platform and tracking the satellite signals without the need for several receivers.

1 INTRODUCTION

The navigation signals received from satellites are so weak that they are drowned in the receiver's thermal noise. Therefore the processing of such signals is susceptible to interfering signals from many kinds of terrestrial sources. The sources may be both intentionally or uninentionally corrupting the satellite navigation signals.

There exist techniques to cope with RF interference and very low power received signals in practically all stages of the receiver. Among them are frontend filter optimization [1], pulse blanking in time or frequency domain [2], multisensor fusion [3], vector tracking [4], digital beamforming [5], Kalman filtering [6], etc. Most of these techniques can be applied independent of each other.

In this paper the focus is on vector tracking and digital beamforming. In the latter the receiver picks up the satellite signals with more than one antenna. The relative phasing of the antenna elements can be digitally chosen such that the wanted signals sum up constructively. In this way the antenna gain can be enhanced for the satellite signal whereas interferences coming from other directions are attenuated [7]. Thus the sensitivity w.r.t. noise is improved.

Multisatellite tracking algorithms – also called vector tracking – exploit the spatial correlation between the received satellite signals in the carrier- and code-phase tracking. This allows a compensation of short signal outages on a few satellites [8]. Especially coherent multisatellite tracking algorithms show promising results, even for standalone positioning [9].

A direct combination of multisatellite tracking and beamforming with multiple antennas is straight-forward as the beamforming is transparent for any later processing stages in the receiver. But the computation of the optimal relative phasing between the antenna elements is typically computation intensive. Additionally when combining the signals from the different antennas before the tracking, the information about their relative position is lost. But this information can be used to determine the spatial orientation of the receiver platform (platform attitude), given the positions of the antenna elements on the platform are known.

Therefore the objective of this paper is to derive a multisatellite multiantenna tracking algorithm. The paper focuses on the inherent determination of the receiver platform attitude inside a multisatellite tracking loop.

The paper is organized as follows: The notation that is used throughout the paper is introduced in the following section 2. The derivation of the algorithm is split into three parts: the derivation of the process model, its application to a linear filter, and finally the inclusion of measurements in the filter. In section 6 the convergence of the derived algorithm is analyzed, followed by a comparison of the multiantenna multisatellite tracking with a traditional digital beamforming. Section 8 presents simulation results before the paper is concluded in section 9.

2 NOTATION

The notation used in this paper mainly follows the notation of [3]. It is repeated here for clarification. Most of the important quantities are also illustrated in Fig. 1.

x^e,y^e,z^e the orthogonal axes of the cartesian e-frame. The Earth-centered Earth-fixed frame (abbreviated ECEF- or e-frame) has its origin in the center of the earth, its z-axis points in the direction of the earth's axis of rotation and the x-axis points towards the intersection of the equator and the zero meridian.

x^n,y^n,z^n the orthogonal axes of the cartesian n-frame. The origin of the local navigation frame (short n-frame) is the reference point of the receiver's platform. The x- and y-axes point towards north and east.

x^b,y^b,z^b the orthogonal axes of the cartesian b-frame. The body-frame (short b-frame) has its origin in the reference point of the receiver's platform. Its axes may be chosen arbitrarily but are attached to the platform.

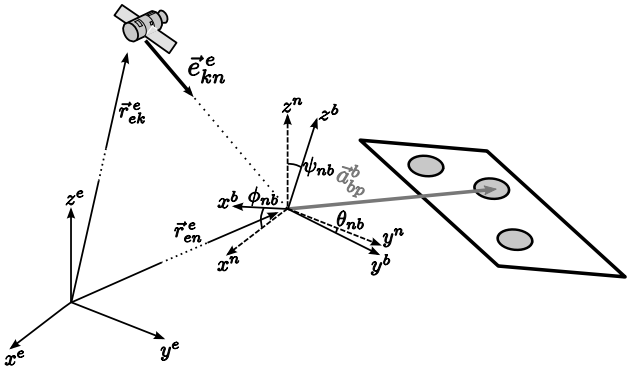

Fig. 1. Spatial vectors used throughout the text.

$\vec{r}^{\,e}_{en} = \vec{r}^{\,e}_{eb}$ the position of the receiver's reference point, described in the e-frame.

$\vec{r}^{\,e}_{ek}$ the position of the k-th satellite, described in the e-frame.

$\vec{e}^{\,e}_{kn} = \vec{e}^{\,e}_{kb}$ the directional vector pointing from satellite k to the receiver platform's reference point, described in the e-frame:

$$\vec{e}^{\,e}_{kn} = \frac{\vec{r}^{\,e}_{en} - \vec{r}^{\,e}_{ek}}{\|\vec{r}^{\,e}_{en} - \vec{r}^{\,e}_{ek}\|}.$$

$\vec{a}^{\,b}_{bp} = \vec{a}^{\,b}_{np}$ the position of the p-th antenna element w.r.t. to the origin of the body-frame (or equivalently the navigation-frame), described in the b-frame.

$\vec{a} \cdot \vec{b} = \vec{a}^{\,T}\vec{b}$ the dot-product between two vectors of the same dimension.

$\phi_{nb}, \theta_{nb}, \psi_{nb}$ roll, pitch and yaw angles (also known as the three Euler angles) describing the attitude of the receiver's platform, i.e. the rotation between the b- and the n-frame.

R^n_b the rotation matrix from the b- to the n-frame, composed by the Euler angles, such that

$$\vec{a}^{\,n}_{bp} = R^n_b \vec{a}^{\,b}_{bp}.$$

q the quaternion describing the same rotation as the three Euler angles. It is defined as

$$q = \begin{pmatrix} \underline{q} \\ q_4 \end{pmatrix} = \begin{pmatrix} \vec{e}_{\mathrm{rot.}} \sin(\gamma/2) \\ \cos(\gamma/2), \end{pmatrix}$$

where $\vec{e}_{\mathrm{rot.}}$ denotes the rotational axis and γ the rotation angle. In principle the quaternion q also needs two indices to denote between which two reference

frames it relates. But for notational brevity this is omitted. Therefore, whenever the rotation (either Euler angles, rotational matrix or quaternion) has no indices, then it corresponds to the rotation from the b-frame to the n-frame, i.e. q_b^n.

$q_1 \otimes q_2$ the quaternion product between the quaternions q_1 and q_2.

$[\omega\times]$ the skew-symmetric matrix of the 3×1 vector ω, defined as

$$[\omega\times] = \begin{pmatrix} 0 & -\omega_3 & \omega_2 \\ \omega_3 & 0 & -\omega_1 \\ -\omega_2 & \omega_1 & 0 \end{pmatrix}.$$

$\delta t, \delta t^k$ the clock offset of the receiver and the k-th satellite w.r.t. system time.

$\mathcal{E}[X]$ the expected value of the random variable X.

$\partial\varphi$ the vector consisting of the process $\varphi(t)$ and all its time-derivatives up to an order $n-1$:

$$\partial\varphi = \begin{pmatrix} \varphi(t) \\ \dot{\varphi}(t) \\ \vdots \\ \dfrac{\partial^{n-1}\varphi(t)}{\partial t^{n-1}} \end{pmatrix}$$

3 SYSTEM DYNAMIC MODEL

In this section the basic equations describing the dynamic behavior of the whole system are derived. A state-space notation will be used throughout the derivation. Basically the receiver motion, the receiver's clock offset, the platform attitude and the carrier-phases of the received signal have to be described.

3.1 Receiver Motion

In derivations for multisatellite tracking algorithms usually all receiver movements are described in the e-frame as it is convenient for most of the involved computations [4]. But in principle any coordinate frame could be used for the descriptions of the receiver position and movements. To later on allow a straight-forward extension to also include inertial sensors, the receiver motion is described in the local navigation- or n-frame, as proposed e.g. in [3]. The six components describing receiver position and velocity are thus[1]: latitude (φ), longitude (λ), height (h), all w.r.t. the earth's reference ellipsoid. Furthermore, velocity in north-, east- and down-direction, i.e. v_n, v_e, v_d.

[1]Receiver position is short for the receiver's reference point position.

The state-space model requires the determination of the time-derivative of the six described parameters w.r.t. time, expressed in terms of themselves. The derivatives can be found in any text-book discussing inertial navigation, e.g. [3]:

$$\begin{pmatrix} \dot{\varphi} \\ \dot{\lambda} \\ \dot{h} \end{pmatrix} = \begin{pmatrix} \dfrac{v_n}{R_n(\varphi)+h} \\ \dfrac{v_e}{(R_e(\varphi)+h)\cos(\varphi)} \\ -v_d \end{pmatrix}, \tag{1}$$

$$\text{with } R_n(\varphi) = \frac{R_e(1-\epsilon^2)}{\left(1-\epsilon^2\sin^2(\varphi)\right)^{3/2}}, \tag{2}$$

$$\text{and } R_e(\varphi) = \frac{R_e}{\sqrt{1-\epsilon^2\sin^2(\varphi)}}. \tag{3}$$

The eccentricity of the earth's ellipsoid is denoted by ϵ. When employing a second order model for the motion of the receiver, like it's done in this paper, the derivative of the velocity components are set to consist simply of the process noise, i.e.

$$\begin{pmatrix} \dot{v}_n \\ \dot{v}_e \\ \dot{v}_d \end{pmatrix} = \begin{pmatrix} w_{v,n} \\ w_{v,e} \\ w_{v,d} \end{pmatrix} = \vec{w}_{v,en}^{\,n}, \tag{4}$$

$$\text{with } \mathcal{E}[w_{v,i}(t)w_{v,i}(t')] = \sigma_{v,i}^2\delta(t-t'),$$

where $i \in \{n, e, d\}$ and $\delta(x)$ the Dirac delta function.

3.2 Receiver Clock

The clock bias of the receiver (w.r.t. system time) can be modeled by an n_δ-th order random walk, e.g. [10]:

$$\begin{pmatrix} c\dot{\delta t} \\ c\ddot{\delta t} \\ \vdots \\ \dfrac{\partial^{n_\delta} c\delta t}{\partial t^{n_\delta}} \end{pmatrix} = \begin{pmatrix} 0 & 1 & 0 & \dots & 0 \\ 0 & 0 & 1 & \dots & 0 \\ \vdots & \vdots & & \ddots & \vdots \\ 0 & 0 & 0 & \dots & 1 \\ 0 & 0 & 0 & \dots & 0 \end{pmatrix} \begin{pmatrix} c\delta t \\ c\dot{\delta t} \\ \vdots \\ \dfrac{\partial^{n_\delta-1} c\delta t}{\partial t^{n_\delta-1}} \end{pmatrix} + \begin{pmatrix} 0 \\ 0 \\ \vdots \\ 1 \end{pmatrix} w_{c\delta},$$

with $\mathcal{E}[w_{c\delta}(t)w_{c\delta}(t')] = \sigma_{c\delta}^2\delta(t-t')$. Actually other noise processes could be included as well, to better model the oscillator noise [10]. In the present derivation this is omitted for notational brevity.

3.3 Receiver Attitude

Like already introduced above, the attitude of the receiver can be described in several ways, including Euler angles,

rotation vectors or quaternions to only name a few (e.g. [11]). In this paper the description of the attitude using quaternions is applied, following [12] and [13].

The time-derivative of the quaternion can be related to the rotation rate ω_{nb}^b (or short just ω), e.g. [14]:

$$\dot{q} = \frac{1}{2}\Omega\left(\omega_{nb}^b\right) q, \text{ with } \Omega(\omega) = \begin{pmatrix} -[\omega\times] & \omega \\ -\omega^T & 0 \end{pmatrix}. \quad (5)$$

Similarly like in the previous section the velocity, the angular velocity of the receiver's platform (w.r.t. the local navigation frame) is described by a white noise process:

$$\dot{\omega}_{nb}^b = \begin{pmatrix} w_{\omega,1} \\ w_{\omega,2} \\ w_{\omega,3} \end{pmatrix} = \vec{w}_\omega,$$

again with $\mathcal{E}\left[w_{\omega,i}(t) w_{\omega,i}(t')\right] = \sigma_{\omega,i}^2 \delta(t-t')$, where $i \in \{1,2,3\}$.

3.4 Carrier-Phase of the Received Signals

It was shown that as a first step to multisatellite carrier-tracking, the carrier-phase processes of the received signals have to be defined [8]. In contrast to the derivations in [8] the model here has to take into account the different antenna elements. The transmitted carrier is simply the nominal carrier plus the clock offset in the satellite, i.e.

$$s^k(t) = \cos\left(\omega_c(t + \delta t^k)\right),$$

where ω_c denotes the (nominal) carrier frequency and δt^k the clock offset of the k-th satellite. The carrier from the k-th satellite received by the p-th antenna element is just the delayed version of the transmitted one, i.e.

$$\begin{aligned} r_p^k(t) &= s^k\left(t - \tau_p^k - \tau_p\right) \\ &= \cos\big(\underbrace{\omega_c(t + \delta t^k - \tau_p^k - \tau_p)}_{\varphi_p^k}\big), \end{aligned}$$

with τ_p^k the propagation delay and τ_p an antenna-element specific constant delay (e.g. due to differences in cable lengths). The propagation delay τ_p^k can be further expressed using the satellite position, $\vec{r}_{ek}^{\,n}$, the position vector of the p-th antenna element $\vec{r}_{ep}^{\,n}$ and the receiver's clock bias δt:

$$\tau_p^k = \frac{1}{c}\left\|\vec{r}_{ep}^{\,n} - \vec{r}_{ek}^{\,n}\right\| + \delta t.$$

This leads to the definition of the carrier-phase $\varphi_p^k(t)$ of the received signal[2]:

$$\begin{aligned} \varphi_p^k(t) &= \omega_c(t-\tau_p) - \frac{2\pi}{\lambda}\Big(\left\|\vec{r}_{ep}^{\,n} - \vec{r}_{ek}^{\,n}\right\| + \left(c\delta t - c\delta t^k\right)\Big) \\ &\approx \omega_c(t-\tau_p) - \frac{2\pi}{\lambda}\Big(\vec{e}_{kn}^{\,n} \cdot \left(\vec{r}_{ep}^{\,n} - \vec{r}_{ek}^{\,n}\right) + \left(c\delta t - c\delta t^k\right)\Big). \end{aligned}$$

Above the wavelength of the carrier is denoted by the symbol λ. The second step is only approximately equal since the used unit vector doesn't point to the particular antenna element but to the reference point of the antenna. But as long as the distances between the antenna elements are considerably smaller than the distance between the receiver and the satellite, it's a very good approximation.

Since the position of the p-th antenna on the receiver's platform is known, the above equation can be rewritten using

$$\vec{r}_{ep}^{\,n} = \vec{r}_{en}^{\,n} + \vec{r}_{np}^{\,n} = \vec{r}_{en}^{\,n} + R_b^n \vec{a}_{bp}^{\,b} = \vec{r}_{en}^{\,n} + R_b^n(q)\vec{a}_{bp}^{\,b}.$$

And thus it can be easily seen that carrier-phase of the k-th satellite signal, picked up by the p-th antenna element consists of a general receiver- and an antenna element-specific part:

$$\begin{aligned} \varphi_p^k(t) &\approx \omega_c t - \frac{2\pi}{\lambda}\Big(\vec{e}_{kn}^{\,n} \cdot \left(\vec{r}_{en}^{\,n} + R_b^n \vec{a}_{bp}^{\,b} - \vec{r}_{ek}^{\,n}\right) \\ &\qquad + \left(c\delta t - c\delta t^k\right)\Big) - \omega_c\tau_p \\ &= \underbrace{\omega_c t + \frac{2\pi}{\lambda}\left(\vec{e}_{kn}^{\,n} \cdot \vec{r}_{ek}^{\,n} + c\delta t^k\right) - \frac{2\pi}{\lambda}\left(\vec{e}_{kn}^{\,n} \cdot \vec{r}_{en}^{\,n} + c\delta t\right)}_{\varphi^k(t)} \\ &\qquad \underbrace{-\frac{2\pi}{\lambda}\vec{e}_{kn}^{\,n} R_b^n \vec{a}_{bp}^{\,b}}_{\psi_p^k(t)} - \underbrace{\omega_c\tau_p}_{-\beta_p(t)}. \end{aligned}$$

As was done for the other processes, the carrier-phase can be written in terms of a state-space model, consisting of the derivatives of the process itself. Care has to be taken at this stage since it directly translates to the estimator later on. One could actually relate the derivatives of the carrier-phase to all involved processes like the receiver position and clock, platform attitude and antenna element bias. But this would only exploit the statistical correlation between all carrier-phase processes and not give access to the estimated quantities themselves. Therefore only the satellite-specific part and the element bias is modeled by a state-space model, the remainder directly relates to the attitude,

[2] For simplicity additional components in the propagation delay like the troposphere or ionosphere are neglected in this derivation. But an extension to also include them is straightforward.

which shall be estimated:

$$\partial\varphi^k = \begin{pmatrix} \dot{\varphi}^k \\ \ddot{\varphi}^k \\ \vdots \\ \frac{\partial^n \varphi^k}{\partial t^n} \end{pmatrix} = \begin{pmatrix} 0 & 1 & 0 & \dots & 0 \\ 0 & 0 & 1 & \dots & 0 \\ \vdots & \vdots & & \ddots & \vdots \\ 0 & 0 & 0 & \dots & 1 \\ 0 & 0 & 0 & \dots & 0 \end{pmatrix} \begin{pmatrix} \varphi^k \\ \dot{\varphi}^k \\ \vdots \\ \frac{\partial^{n-1} \varphi^k}{\partial t^{n-1}} \end{pmatrix} - \frac{2\pi}{\lambda} \begin{pmatrix} 0 & 0 \\ (\vec{e}^{\,e}_{kn})^T & 0 \\ 0 & 0 \\ \vdots & \vdots \\ 0 & 1 \end{pmatrix} \begin{pmatrix} \vec{w}^{\,n}_{v,en} \\ w_\delta \end{pmatrix} + \frac{2\pi}{\lambda} \begin{pmatrix} 0 & 0 \\ (\vec{e}^{\,e}_{kn})^T & 1 \\ 0 & 0 \\ \vdots & \vdots \end{pmatrix} \begin{pmatrix} \ddot{\vec{r}}^{\,e}_{ek} \\ c\ddot{\delta}t^k \end{pmatrix} \quad (6)$$

The antenna-element delay β_p is modeled as a bias and thus constant. It's state-space description simply reads

$$\dot{\beta}_p = w_{\beta_p}.$$

4 FILTERING

The process model derived in the previous section can now be used to drive a filter. In the present setup a Kalman filter is employed. The process of the receiver motion and platform attitude have a nonlinear model, a linearization is thus needed in those cases. A straightforward linearization about the current estimate can be obtained by formulating the filter as an error-state filter. This means that instead of the actual quantities themselves, the filter estimates the difference between the true values and their estimates.

For a state-vector x and a non-linear dynamic model $f(x)$ the error-state filter can be easily derived as follows (w the process noise):

$$\dot{x} = f(x) + Gw \quad (7)$$

$$\approx f(\hat{x}) + \frac{\partial f(\hat{x})}{\partial x}(x - \hat{x}) + Gw. \quad (8)$$

If $\hat{x}$ is the filter's estimate of the state-vector x then it can be rewritten as a (nonlinear) process as well:

$$\dot{\hat{x}} = f(\hat{x}). \quad (9)$$

Of course the filter does not add noise and therefore the second term in Eq. (7) has to be omitted in the model of the estimate. Plugging Eq. (8) into Eq. (9) the error-state process model is found:

$$\text{with } \Delta x = x - \hat{x}\text{:}$$

$$\Delta\dot{x} = \frac{\partial f(\hat{x})}{\partial x}\Delta x + Gw.$$

It can easily be seen that the above steps can also be applied if the process model is linear, which is e.g. the case for the carrier-phase φ^k.

4.1 Receiver Motion

The process model for the receiver motion, outlined in section 3.1, can now be linearized to find the error-state process model. A description of the receiver position using longitude, latitude and height is disadvantageous in terms of numerical stability, therefore the position offset is translated to an east- and north-error [15]:

$$\Delta r_n \approx \left(R_n(\hat{\varphi}) + \hat{h}\right)\Delta\varphi,$$
$$\Delta r_e \approx \left(R_e(\hat{\varphi}) + \hat{h}\right)\cos(\hat{\varphi})\Delta\lambda,$$

with the functions $R_n(.)$ and $R_e(.)$ as already defined in Eqs. (2) and (3). Compiling Eqs. (1) and (4) with the above two definitions results in

$$\begin{pmatrix} \Delta\dot{\vec{r}}^{\,n}_{en} \\ \Delta\dot{\vec{v}}^{\,n}_{en} \end{pmatrix} = \begin{pmatrix} F_r & I_3 \\ 0_{3,3} & 0_{3,3} \end{pmatrix} \begin{pmatrix} \Delta\vec{r}^{\,n}_{en} \\ \Delta\vec{v}^{\,n}_{en} \end{pmatrix} + \begin{pmatrix} 0_{3,3} \\ I_3 \end{pmatrix} \vec{w}^{\,n}_{v,en},$$

$$\text{with } F_r = \begin{pmatrix} 0 & 0 & \frac{\hat{v}_n}{R_n(\hat{\varphi})+\hat{h}} \\ \frac{\hat{v}_e \tan(\hat{\varphi})}{R_n(\hat{\varphi})+\hat{h}} & 0 & \frac{\hat{v}_e}{R_e(\hat{\varphi})+\hat{h}} \\ 0 & 0 & 0 \end{pmatrix},$$

I_n the identity matrix of dimension $n \times n$ and $0_{m,n}$ an all-zeros matrix of dimension $m \times n$.

4.2 Attitude

It was already mentioned above that in this derivation the quaternion attitude representation is used. The linearization of the process model for an error-state filter is not straightforward for the attitude, because of the nature of the quaternion. The quaternion representation of the attitude is overdetermined (due to its four parameters, but only three spatial rotation axes). To be valid it must always be of unit length. A basic linearization doesn't take this condition into account. The problem could be solved, like in [13], by applying a small-angle approximation and only estimating the first three components of the error-quaternion and choosing the fourth such that unit length results.

The solution applied in this paper follows [12], where the error-quaternion is parametrized by the three-components vector α:

$$\Delta q = \frac{1}{\sqrt{4 + \|\alpha\|^2}} \begin{pmatrix} \alpha \\ 2 \end{pmatrix}.$$

The true rotation matrix can now be written to be composed of the estimated quaternion $\hat{q}$ and the error quaternion Δq:

$$R(q) = R(\Delta q \otimes \hat{q}) = R(\Delta q)R(\hat{q}) \;\Rightarrow\; \Delta q = q \otimes \hat{q}^{-1},$$

where $\hat{q}^{-1}$ denotes the inverse quaternion of $\hat{q}$. What remains is the computation of the derivative of vector α. In a first step the derivative of the error-quaternion Δq is determined:

$$\begin{aligned}\Delta\dot{q} &= \frac{\partial}{\partial t}\left(q \otimes \hat{q}^{-1}\right) \\ &= \dot{q} \otimes \hat{q}^{-1} + q \otimes \frac{\partial \hat{q}^{-1}}{\partial t} \\ &= \frac{1}{2}\Omega(\omega) q \otimes \hat{q}^{-1} - q \otimes \hat{q}^{-1} \otimes \dot{\hat{q}} \otimes \hat{q}^{-1}.\end{aligned}$$

In the last step Eq. (5) was used together with the identity

$$\frac{\partial q^{-1}}{\partial t} = -q^{-1} \otimes \dot{q} \otimes q^{-1}.$$

With some further simplifying steps it can be shown that

$$\Delta\dot{q} = \frac{1}{2}\begin{pmatrix} -\left[(\omega + \hat{\omega})\times\right] & \omega - \hat{\omega} \\ -(\omega - \hat{\omega}^T) & 0 \end{pmatrix} \Delta q. \qquad (10)$$

It can easily be seen that $\alpha = 2\Delta\underline{q}/\Delta q_4$. And so

$$\dot{\alpha} = 2\frac{\Delta\dot{\underline{q}}\Delta q_4 - \Delta\underline{q}\Delta\dot{q}_4}{\Delta q_4^2}.$$

With Eq. (10) the above derivative can be expressed in terms of α, $\Delta\omega$ and $\hat{\omega}$ only:

$$\dot{\alpha} = -\frac{1}{2}\left[\Delta\omega\times\right]\alpha - \left[\hat{\omega}\times\right]\alpha + \Delta\omega + \frac{1}{4}\left(\Delta\omega^T\alpha\right)\alpha.$$

Due to the first and fourth summand the above equation is nonlinear. It has to be linearized as well, like already shown for the receiver motion. Since α parametrizes the error quaternion such that when α equals zero $q = \hat{q}$, it is evident that the linearization takes place around $\alpha = 0$. And so the linearized error-state process model for the attitude part is found to read[3]

$$\begin{pmatrix}\dot{\alpha} \\ \Delta\dot{\omega}\end{pmatrix} \approx \begin{pmatrix} -\left[\hat{\omega}\times\right] & I_3 \\ 0_{3,3} & 0_{3,3}\end{pmatrix}\begin{pmatrix}\alpha \\ \Delta\omega\end{pmatrix} + \begin{pmatrix}0_{3,3} \\ I_3\end{pmatrix} w_\omega.$$

4.3 Carrier-Phase of the Received Signals

In the case of the carrier-phase also an error-state filtering approach is applied. In this case not because of the nonlinearity of the process model but instead due to the availability of error-measurements. It will be derived in the next section that the carrier-phase measurements can be directly related to the carrier-phase error-state.

In addition to the process noise the error-state of the carrier-phase also has a control signal as input. The control signal originates from the model of the NCO which offers typically a steering of the carrier-phase and carrier-frequency of the local replica (i.e. synonym for estimate of the carrier-phase and its first derivative):

$$\partial\Delta\dot{\varphi}^k = F_{\varphi,n}\partial\Delta\varphi^k + B_\varphi u_{\varphi^k} + G_\varphi w_{\varphi^k},$$

where $F_{\varphi,n}$ is a block-matrix consisting of all-zeros matrices and an identity matrix

$$F_{\varphi,n} = \begin{pmatrix} 0_{n-1,1} & I_{n-1} \\ 0 & 0_{1,n-1}\end{pmatrix}$$

like already used in Eq. (6). The control input matrix B_φ is defined like in [8]. The input u_{φ^k} is computed such that the local carrier replica stays synchronized with the received signal. Typically a linear controller is employed:

$$u_{\varphi^k} = -L_\varphi\partial\Delta\varphi^k.$$

More information about how to compute L_φ can be found in any textbook on control theory or short in [9].

4.4 State-Vector

The first steps outlined above allow now to compile a reasonable state-vector for the desired application. The state-vector x is setup to consist of the error-state in the position and velocity of the receiver, the receiver's clock (and its derivatives), the attitude error and the corresponding angular rate error, the antenna element bias errors and finally the carrier-phase errors:

$$x = \begin{pmatrix} \Delta\vec{r}^{\,n}_{en} \\ \Delta\vec{v}^{\,n}_{en} \\ \alpha \\ \Delta\omega^b_{nb} \\ \partial c\Delta\delta t \\ \Delta\beta_1 \\ \vdots \\ \Delta\beta_P \\ \partial\Delta\varphi^1 \\ \vdots \\ \partial\Delta\varphi^K \end{pmatrix} \qquad (11)$$

5 MEASUREMENTS

What finally remains to implement the filter is the description of how the measurements relate to the state-vector, defined in Eq. (11). In spread spectrum systems two measurements can be used, which are the carrier-phase and code-phase discriminator outputs. Both measurements contain the projection of the vector to the antenna elements onto the line-of-sight vector. This is first derived followed by further explanations about the measurements.

[3] As explained further above, the angular rate ω actually possesses indices ω^b_{nb}. They are omitted for notational simplicity.

5.1 Projection of a Rotated Vector

In the relationship between the code- and carrier-phase measurements and the state-vector, the projection of the antenna-element vector $\vec{a}_{np}^{\,b}$ onto the line-of-sight link to the satellite shows up. In a first step this projection is derived. For any given vectors $\vec{a}$ and $\vec{b}$ of dimension 3×1, the difference between true and estimated projection reads

$$\begin{aligned}\Delta P(\vec{a}\,,\vec{b}\,) &= \vec{a}\,\cdot R(q)\vec{b}\, - \vec{a}\,\cdot R(\hat{q})\vec{b}\\ &= \vec{a}^{\,T} R(q)\vec{b}\, - \vec{a}^{\,T} R(\hat{q})\vec{b}\,.\end{aligned}$$

Like previously the true quaternion can be defined as the product of an error quaternion Δq and the estimated quaternion $\hat{q}$:

$$\Delta P(\vec{a}\,,\vec{b}\,) = \vec{a}^{\,T}\Big(R(\Delta q) - I_3\Big)R(\hat{q})\vec{b}\,.$$

Applying the definition of the rotation matrix for a quaternion and the parametrization of Δq by the vector α, it's easy to show that

$$\begin{aligned}R(\Delta q) - I_3 = \frac{1}{4 + \|\alpha\|^2}\Big(&-2\,\|\alpha\|^2 I_3\\ &+ 2\alpha\alpha^T - 4\,[\alpha\times]\Big).\end{aligned}$$

By using the Binet-Cauchy identity the projection can finally be found as

$$\begin{aligned}\Delta P(\vec{a}\,,\vec{b}\,) = \frac{1}{4 + \alpha^T\alpha}\Big(&2\alpha^T\,[\vec{a}\,\times]\Big[R(\hat{q})\vec{b}\,\times\Big]\,\alpha\\ &+ 4\vec{a}^{\,T}\Big[R(\hat{q})\vec{b}\,\times\Big]\,\alpha\Big).\end{aligned}$$

Clearly the above equation is quadratic due to the first summand. A linearization can be thus performed for the measurement equation as well. Of course, it's again reasonable to linearize around $\alpha = 0$:

$$\begin{aligned}\Delta P(\vec{a}\,,\vec{b}\,) &\approx \Delta P(\vec{a}\,,\vec{b}\,)\Big|_{\alpha=0} + \Big(\nabla_\alpha \Delta P(\vec{a}\,,\vec{b}\,)\Big|_{\alpha=0}\Big)\,\alpha\\ &= \vec{a}^{\,T}\Big[R(\hat{q})\vec{b}\,\times\Big]\,\alpha. \qquad (12)\end{aligned}$$

5.1.1 Time-Derivative

Since the attitude is typically modeled as a second order process, the derivative of the above projection needs to be evaluated as well. Assuming that the two vectors $\vec{a}$ and $\vec{b}$ are constant over time, only the derivative of the rotation matrix needs to be considered:

$$\Delta\dot{P}(\vec{a}\,,\vec{b}\,) = \vec{a}^{\,T}\Big(\dot{R}(q) - \dot{R}(\hat{q})\Big)\,\vec{b}\,.$$

The derivative can be expressed in terms of the rotation matrix itself and the skew matrix of the rotation rate vector [15]:

$$\Delta\dot{P}(\vec{a}\,,\vec{b}\,) = \vec{a}^{\,T}\Big(R(q)\,[\omega\times] - R(\hat{q})\,[\hat{\omega}\times]\Big)\vec{b}\,.$$

By noting that $\omega = \Delta\omega + \hat{\omega}$ the above derivative can further be expanded into

$$\begin{aligned}\Delta\dot{P}(\vec{a}\,,\vec{b}\,) = \vec{a}^{\,T}\Big(&R(q)\,[\Delta\omega\times] + R(q)\,[\hat{\omega}\times]\\ &- R(\hat{q})\,[\hat{\omega}\times]\Big)\vec{b}\,.\end{aligned}$$

A similar linearization like in the derivation for Eq. (12) can be applied to result in

$$\begin{aligned}\Delta\dot{P}(\vec{a}\,,\vec{b}\,) \approx\ &\vec{a}^{\,T}\Big[R(\hat{q})\,[\hat{\omega}\times]\,\vec{b}\,\times\Big]\,\alpha\\ &- \vec{a}^{\,T}R(\hat{q})\Big[\vec{b}\,\times\Big]\,\Delta\omega. \qquad (13)\end{aligned}$$

5.2 Code-Phase

The code-phase discriminator returns for a particular satellite signal the difference between the code-phase of the received signal and the local replica:

$$D_{\tau,p}^k \approx c\tau_p^k - c\hat{\tau}_p^k + v_{\tau,p}^k.$$

The time-index is neglected here to shorten the notation. Above τ_p^k denotes the code-phase of the signal received from satellite k by the p-th antenna element. Similarly $\hat{\tau}_p^k$ denotes the code-phase of the local replica for the corresponding signal. The measurement noise is denoted by $v_{\tau,p}^k$. With this notation the code-phase τ_p^k is equivalent to the propagation delay:

$$\begin{aligned}D_{\tau,p}^k &\approx \left\|\vec{r}_{ep}^{\,n} - \vec{r}_{ek}^{\,n}\right\| + c\left(\delta t - \delta t^k\right)\\ &\quad - \left\|\hat{\vec{r}}_{ep}^{\,n} - \vec{r}_{ek}^{\,n}\right\| - c\left(\hat{\delta t} - \delta t^k\right) + v_{\tau,p}^k\\ &\approx \hat{\vec{e}}_{kn}^{\,n}\cdot\left(\vec{r}_{ep}^{\,n} - \hat{\vec{r}}_{ep}^{\,n}\right) + c\left(\delta t - \hat{\delta t}\right) + v_{\tau,p}^k\\ &= \hat{\vec{e}}_{kn}^{\,n}\cdot\left(\Delta\vec{r}_{en}^{\,n} + [R_b^n(\Delta q) - I_3]\,R_b^n(\hat{q})\vec{a}_{np}^{\,b}\right)\\ &\quad + c\Delta\delta t + v_{\tau,p}^k\end{aligned}$$

The summand containing the rotation matrix R_b^n can be replaced by the linearization derived in the previous section, Eq. (12):

$$D_{\tau,p}^k \approx \hat{\vec{e}}_{kn}^{\,n}\cdot\Delta\vec{r}_{en}^{\,n} + \hat{\vec{e}}_{kn}^{\,n}\cdot\left[R_b^n(\hat{q})\vec{a}_{np}^{\,b}\times\right] + c\Delta\delta t + v_{\tau,p}^k.$$

Whenever the wavelength of the spreading code is considerably larger than the distance between the antenna elements, i.e. $\|\vec{a}_{np}^{\,b} - \vec{a}_{np'}^{\,b}\| \ll c/f_{\mathrm{code}}\ \forall p, p'$, then the second summand could be neglected. This would imply that the information about the attitude is only determined from the carrier-phase measurements.

5.3 Carrier-Phase

It was shown in [6] that the carrier-phase discriminator outputs the average carrier-phase error over the correlation in-

terval:

$$
\begin{aligned}
D^k_{\varphi,p} &\approx \overline{\Delta\varphi^k_p} + v^k_{\varphi,p} \qquad (14)\\
&= \overline{\Delta\varphi^k} + \overline{\Delta\psi^k_p} + \Delta\beta_p + v^k_{\varphi,p}\\
&= \Delta\varphi^k + \frac{T}{2}\Delta\dot{\varphi}^k + \frac{T^2}{6}\Delta\ddot{\varphi}^k \ldots\\
&\quad + \Delta\psi^k_p + \frac{T}{2}\Delta\dot{\psi}^k_p + \ldots + \Delta\beta_p + v^k_{\varphi,p}
\end{aligned}
$$

The attitude part, described by the $\Delta\psi^k_p$-terms can be simplified using the results of Eq. (12) and (13):

$$
\begin{aligned}
\Delta\psi^k_p &= -\frac{2\pi}{\lambda}\,\hat{\vec{e}}^n_{kn}\cdot\left[R^n_b(\hat{q})\vec{a}^{\,b}_{np}\times\right]\alpha,\\
\Delta\dot{\psi}^k_p &= -\frac{2\pi}{\lambda}\Big(\hat{\vec{e}}^n_{kn}\cdot\left[\left(R^n_b(\hat{q})\left[\hat{\omega}^b_{nb}\times\right]\vec{a}^{\,b}_{np}\right)\times\right]\alpha\\
&\qquad - \hat{\vec{e}}^n_{kn}\cdot R^n_b(\hat{q})\left[\vec{a}^{\,b}_{np}\times\right]\Delta\omega\Big).
\end{aligned}
$$

Since the attitude is modeled as a second order process, only the terms up to the first derivative are considered. Finally the relationship between the satellite-dependent part φ^k and the state-vector can be found in [8].

6 CONVERGENCE

In the previous sections 3, 4 and 5 the basic state-space model was derived. It is ready to be implemented by any linear filtering algorithm. For example the Kalman filter tries to find the optimal solution for the above model in terms of maximum likelihood.

Due to the linearization in the attitude computations, the filter may not converge to the true solution. This is best illustrated in Fig. 2. The cost function given by the squared norm between the carrier-phase measurements and their corresponding estimates is plotted for erroneous first and second component of the quaternion q, i.e. $\hat{q}_1$ and $\hat{q}_2$. The white space outside the unit circle is simply the area for which a valid quaternion could not be found and thus has to be neglected in the plot. The true quaternion was the identity quaternion, i.e. $q_1 = q_2 = 0$. It can be seen that the cost function is not convex and thus whenever the filter is initialized with a quaternion not being close to the true one, the filter may not converge to the true solution.

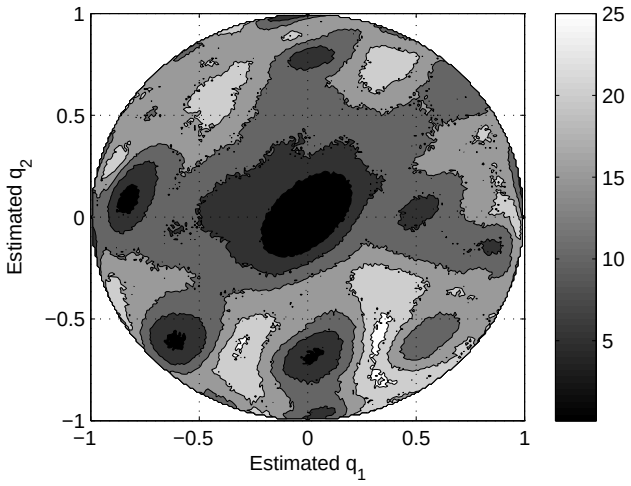

Fig. 2. Cost function $J = \|y - \hat{y}\|^2$, given all variables are known except the first two components of the quaternion (q_1, q_2).

Thus it is important to be able to detect whether or not the filter has converged to the global optimum. A way how to detect a wrong convergence is proposed in the next section.

6.1 Convergence Test

The major convergence problem emerges from the attitude determination. Since in a typical setup the distances between the antenna elements is considerably smaller than the length of a chip of the spreading code, the focus here is put to the carrier-phase measurements.

Previously it was shown that the carrier-phase measurements can be related to the state-vector, see Eq. (14). This relationship is generally nonlinear

$$
\begin{aligned}
D_\varphi &= \left(D^1_{\varphi,1}, \quad D^2_{\varphi,1}, \quad \ldots, \quad D^K_{\varphi,P}\right)^T\\
&= H_\varphi(x) + v_\varphi,\\
&\text{with } \mathcal{E}\left[v_\varphi\right] = 0 \text{ and } \mathcal{E}\left[v_\varphi v_\varphi^T\right] = R.
\end{aligned}
$$

The filter's estimate of the measurement vector correpsondingly reads

$$\hat{D}_\varphi = H_\varphi(\hat{x}).$$

Thus the measurement residual can be linearly approximated:

$$
\begin{aligned}
\Delta D_\varphi &= D_\varphi - \hat{D}_\varphi\\
&\approx H_\varphi(\hat{x}) + \nabla_x H_\varphi(\hat{x})(x - \hat{x}) - H(\hat{x}) + v_\varphi\\
&= \nabla_x H_\varphi(\hat{x})(x - \hat{x}) + v_\varphi.
\end{aligned}
$$

The gradients have already been evaluated in the previous section, in which the measurements were introduced (section 5). Since the state estimation error $e = x - \hat{x}$ is approximately Gaussian distributed, the carrier-phase residual $\Delta D_\varphi = D_\varphi - \hat{D}_\varphi$ is also approximately Gaussian distributed with mean

$$\mathcal{E}\left[\Delta D_\varphi\right] \approx \mathcal{E}\left[\nabla H_\varphi(\hat{x})e\right] + \mathcal{E}\left[v_\varphi\right] = 0 \qquad (15)$$

and covariance

$$
\begin{aligned}
\operatorname{cov}\left[\Delta D_\varphi\right] &\approx \mathcal{E}\left[\left(\nabla H_\varphi(\hat{x})e + v_\varphi\right)\left(\nabla H_\varphi(\hat{x})e + v_\varphi\right)^T\right]\\
&= \nabla H_\varphi(\hat{x}) P H^T_\varphi(\hat{x}) + R, \qquad (16)
\end{aligned}
$$

with $P = \mathcal{E}\left[ee^T\right]$ the state estimation error covariance matrix, as used e.g. in the Kalman filter. Therefore if the filter has converged to the true state, the state estimation error is thus zero-mean:

$$\Delta D_\varphi \sim \mathcal{N}\left(0,\ \nabla H_\varphi(\hat{x}) P \nabla H_\varphi^T(\hat{x}) + R\right).$$

Therefore the normalized sum of squared errors is proposed to test whether or not the filter has converged to the true attitude:

$$\Delta D_{\varphi,\text{norm.}} = \left(\nabla H_\varphi(\hat{x}) P \nabla H_\varphi^T(\hat{x}) + R\right)^{-\frac{1}{2}} \Delta D_\varphi \quad (17)$$
$$\Rightarrow\ \text{WSSE}_\varphi = \left\|\Delta D_{\varphi,\text{norm.}}\right\|^2 \sim \chi^2_{(KP)}.$$

Above the square-root of a matrix is defined as $A^{-\frac{1}{2}} A^{-\frac{1}{2}} = A^{-1}$, which could be obtained e.g. by an eigenvalue decomposition.

Since by definition the additive measurement noise v_φ is zero-mean, Eq. (15) requires that

$$\nabla H_\varphi(\hat{x})\, \mathcal{E}\left[e\right] = 0.$$

This equation can only be fulfilled if $\mathcal{E}\left[e\right] \in \text{Ker}\left(\nabla H_\varphi(\hat{x})\right)$. The trivial solution, i.e. $\mathcal{E}\left[e\right] = 0$ is, of course, the targeted correct solution, i.e. convergence to the global optimum. It can be noted that[4] [16]

$$\text{since } \nabla H_\varphi(\hat{x}):\ (KP) \times (3+3+P+nK)$$
$$\dim\left(\text{Ker}\left(\nabla H_\varphi(\hat{x})\right)\right) = (3+3+P+nK) - \text{rank}\left(\nabla H_\varphi(\hat{x})\right).$$

But the rank of a matrix cannot be larger than the number of rows or the number of columns. Therefore the rank of the matrix $\nabla H_\varphi(\hat{x})$ is

$$\text{rank}\left(\nabla H_\varphi(\hat{x})\right) \leq \min\left(KP,\ 3+3+P+nK\right).$$

For a typical case with a 2×2 antenna array (i.e. $P = 4$), when at least five satellites are visible (i.e. $K \geq 5$), then

$$\text{rank}\left(\nabla H_\varphi(\hat{x})\right) \leq 3+3+P+nK.$$

In a non-degenerate configuration, the above inequality reduces to equality. Consequently the dimension of the kernel of $\nabla H_\varphi(\hat{x})$ is zero and as such Eq. (15) has only the trivial solution. This means that the norm of the weighted residuals is χ^2-distributed if and only if the global optimum has been found. Thus the binary decision whether or not the global optimum is reached is proposed as

decide global optimum iff
$\text{WSSE}_\varphi < \chi^2_{1-s}(KP)$ at
significance level s.

[4] without loss of generality for this short analysis the position and clock bias of the receiver are neglected, as they are mainly determined by the code-phase measurements (which are not considered in this convergence discussion).

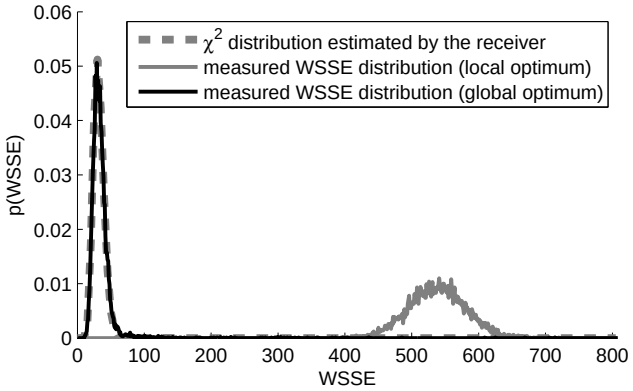

Fig. 3. Test statistic (WSSE), simulations vs. theory.

An exemplary illustration of the above test is shown in Fig. 3. What can be seen is an excellent fit of the WSSE distribution for the global optimum. Furthermore a convergence to a wrong attitude solution leads to a substantial offset in the distribution and can clearly be identified by the described test.

Of course, the appropriate normalization of the residuals in Eq. (17) is a crucial step in the decision. An accurate estimation of the measurement and state estimation error covariance matrix is needed, i.e. R and P respectively. It was shown that especially the estimation of the latter is difficult due to the unknown or potentially unprecise model of the process noise [17]. There exist a few approaches which allow an online determination of the state estimation error covariance matrix. For more details consider the overview in [18].

6.2 Reinitialization

Together with a test of convergence, a scheme for reinitializing the attitude solution is needed. A brute-force grid search is inefficient in this case. Therefore an exemplary reinitialization scheme is proposed here to result in a fast and reliable convergence to the true attitude.

The initial attitude description is defined by the rotation axis and a corresponding angle of rotation. The rotation axis alternately points from the origin towards the vertices of a cube centered at $(0,0,0)^T$:

$$\vec{e}_{\text{rot.},m} = \frac{1}{\sqrt{3}} \begin{pmatrix} (-1)^{\lfloor \frac{m}{2} \rfloor} \\ (-1)^{\lfloor \frac{m}{2} \rfloor + \lfloor \frac{k}{4} \rfloor} \\ (-1)^m \end{pmatrix},\ \text{for } m = 0, 1, \ldots, 7.$$

The rotation angle is defined as fractions of 2π:

$$\zeta_{i,\ell} = 2\pi \left(\frac{1}{2^{i+1}} + \frac{\ell}{2^i}\right),\ \ell = 0, 1, \ldots, 2^i - 1.$$

And so the initial quaternion reads

$$q_{i,\ell,m} = \begin{pmatrix} \vec{e}_{\mathrm{rot.},m} \sin(\zeta_{i,\ell}/2) \\ \cos(\zeta_{i,\ell}/2) \end{pmatrix},$$

with the indices $i = 0, 1, 2, \ldots$, $\ell = 0, 1, \ldots, 2^i - 1$ and $m = 0, 1, \ldots, 7$. The first initial quaternion is $q_{0,0,0}$. Whenever convergence is not achieved, the next is tested. In this way convergence is achieved with only a few reinitializations (simulations indicate on average five).

7 COMPARISON WITH DIGITAL BEAMFORMING

Traditionally a multiantenna receiver exploits the spatial degrees of freedom by applying beamforming to the signals received by the different antenna elements. In the multiantenna multisatellite tracking receiver, the spatial correlation is also exploited, but differently. In this section the two approaches are compared.

One central task of the GNSS receiver is to measure carrier-phases and pseudoranges. Since the carrier-phase estimation is usually more sensitive to noise, its performance is analyzed in the comparison of the two multiantenna signal processing approaches.

For the comparison the signal received at the p-th antenna element is composed of three parts:

$s_p^k(t)$ the wanted signal from satellite k, impacting with power C^k, azimuth and elevation angles A^k and E^k.

$n_{p,0}(t)$ a white thermal noise with spectral density N_0 uncorrelated among the antenna elements.

$n_{p,d}(t)$ a directive white noise, with spectral density N_d, with azimuth angle A_d and elevation angle E_d.

In the numerical examples a planar 2×2 antenna array is used, as illustrated in Fig. 8.

7.1 Digital Beamforming Receiver

Prior to beamforming, the received signals from the different antenna elements are mixed to baseband. For one specific time-instant t the baseband samples from all P antennas $(y_1(t), \ldots, y_P(t))$ are stacked into one complex-valued vector, which is multiplied with the Hermitian transpose of the steering vector w:

$$y(t) = w^H \begin{pmatrix} y_1(t) \\ y_2(t) \\ \vdots \\ y_P(t) \end{pmatrix},$$

with $w^H = (w_1^*,\ w_2^*,\ \ldots,\ w_P^*)$. The baseband signal $y(t)$ is then processed by the receiver using standard tracking loops. This procedure is graphically illustrated in Fig. 4. A

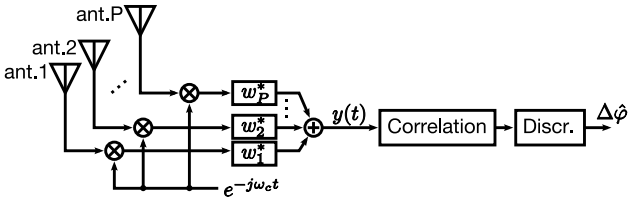

Fig. 4. Digital beamforming in GNSS.

large amount of literature is dedicated to the calculation of the steering vector w [7]. It can be chosen to optimize the receiver performance for the different received signals. For example the weights could be chosen such that the gain for the satellite signal is highest. Or such that interfering signals are best suppressed.

The baseband signal $y(t)$ is finally correlated in the tracking loops with a local replica of the spreading code. Subsequently the correlation result is processed in the carrier-phase discriminator[5]. In [19] it was shown that the amount of noise contained in the discriminator output directly relates to the tracking performance of the receiver. Therefore the variance of the discriminator output is considered as the figure of merit for the comparison.

For a particular satellite azimuth and elevation angle, Fig. 5 shows the variance of the discriminator output (in locked state) for a deterministic beamforming, where the antenna is directed towards the satellite. It can be seen from the illustration that the antenna pattern has its maximum where the satellite is located. This means that the satellite signal is amplified. Furthermore directive noise is strongly attenuated when its indicent angle is not close to the one of the satellite signal. Of course, the weights could be computed in many different ways. But since the multiantenna tracking receiver is striving after a correlation where the local replica perfectly matches the received signals, a comparison with the above described deterministic beamforming is considered to be fair.

7.2 Multiantenna Tracking

It was already described above that the multiantenna tracking receiver correlates the signals from every antenna element individually with local replicas. Consequently for every antenna element and every satellite signal one discriminator is employed. Later on when the phase-offset is estimated – be it in a multisatellite tracking loop or not – the discriminators are combined, according to the Kalman

[5] also called error detector.

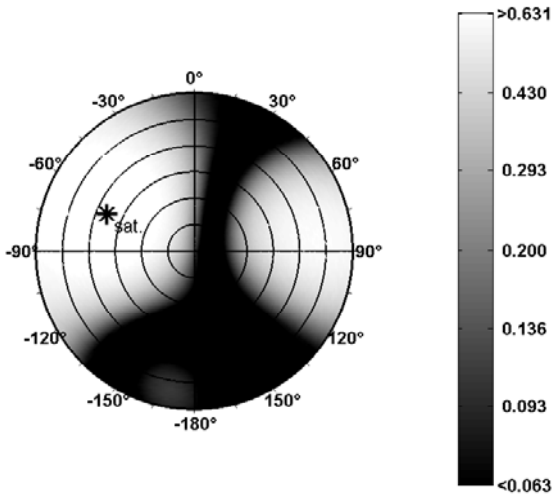

Fig. 5. Variance of the carrier-phase error estimate $\Delta\hat{\varphi}$ in a beamforming receiver. The satellite has azimuth and elevation angles of $A^k = -67°$, $E^k = 36°$ respectively, $C/N_0 = 45$dB-Hz, $N_d = N_0 + 15$dB.

gain. If one satellite signal is received with approximately the same signal-to-noise ratio at every antenna element, then the Kalman gain will be equal for every measurement. And since the estimated phase-offset has to result, the Kalman gain for the projection of the discriminators to the phase-offset is consequently $1/P$ (P the number of antenna elements). This sequence is illustrated in Fig. 6.

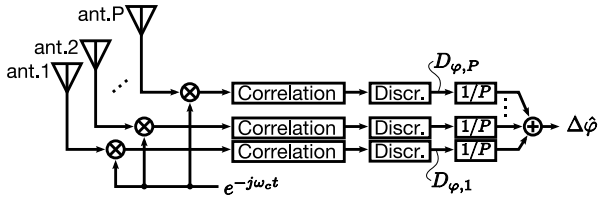

Fig. 6. Processing chain for the multiantenna tracking receiver.

The block diagram depicts the difference to the traditional multiantenna receiver which applies digital beamforming. Of course, the benefit from the combination of the discriminators is the additional possibility to inherently estimate the platform attitude. On the other hand, the drawback is the low flexibility and potential for suppressing interfering signals. This can also be seen from Fig. 7, where the same scenario as in Fig. 5 was evaluated.

Again the maximum is reached for the direction of the satellite which is obvious. But the maximum is not as high as in the case of beam-forming which stems from the fact that the discriminator is a nonlinear operation in the additive noise. And therefore the exchange of summation and discrimination is not possible.

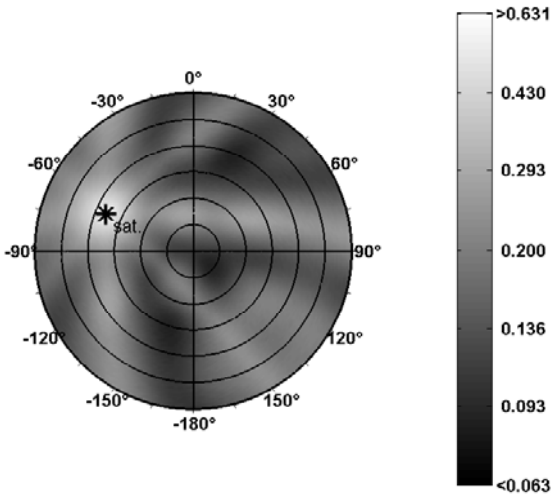

Fig. 7. Variance of the carrier-phase error estimate $\Delta\hat{\varphi}$ in a multiantenna tracking receiver. The satellite has azimuth and elevation angles of $A^k = -67°$, $E^k = 36°$ respectively, $C/N_0 = 45$dB-Hz, $N_d = N_0 + 15$dB.

8 SIMULATION RESULTS

The derived multiantenna multisatellite tracking algorithm could be tested with real measurement data or with simulations. To solely analyze the novel algorithm and for a proof of concept simulations were used. In this way all effects that do not directly relate to the algorithm under test could be avoided. In the simulation IF samples were generated for a planar 2×2 antenna array, as illustrated in Fig. 8. A

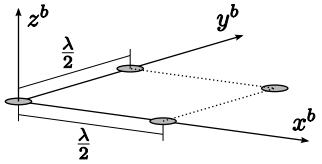

Fig. 8. Antenna array configuration.

similar simulation program was used like documented in [20]. It was extended to additionally simulate multiple antennas. In the simulations no atmospheric effects and no multipath propagation were considered.

A constellation with seven satellites was simulated, where the satellite signals were received with $45\,\mathrm{dB-Hz}$. The two-sided frontend passband bandwidth was $4\,\mathrm{MHz}$, the number of bits in the quantization 4.

8.1 Attitude

The novelty of the multiatenna multisatellite tracking is the inherent estimation of the platform attitude. This is analyzed in Fig. 9. The upper figure shows that the al-

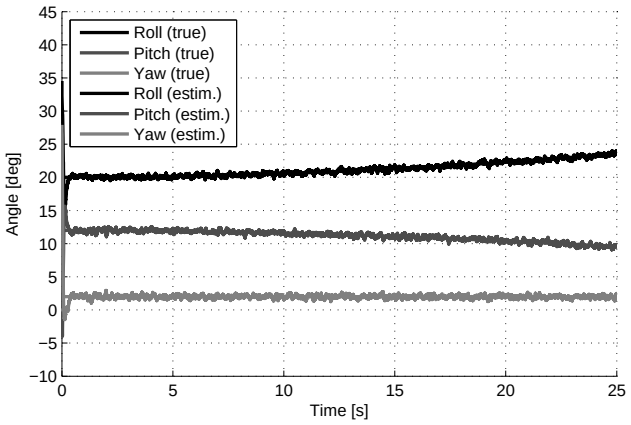

(a) True and estimated attitude.

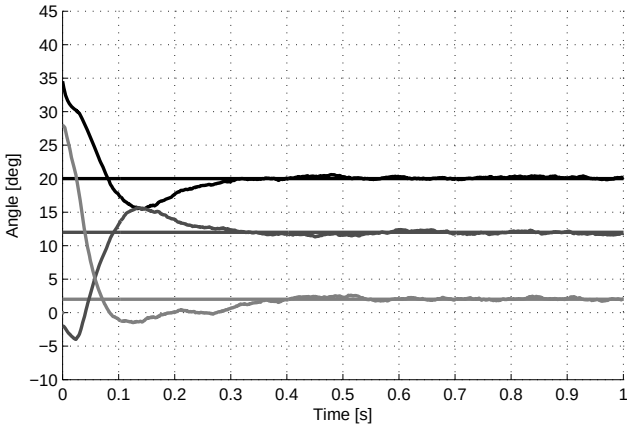

(b) Initial convergence.

Fig. 9. Analysis of the estimated platform attitude.

gorithm can perfectly track the platform attitude, whereas Fig. 9(b) indicates a fast convergence of the attitude estimation. The attitude was initialized wrong by $\Delta\phi_{nb} = 15°$, $\Delta\theta_{nb} = -14°$, $\Delta\psi_{nb} = 26°$, but still the attitude solution converged in less than a second.

8.2 Carrier-Phase Tracking

It is important that the multiantenna tracking does not impair the actual carrier-phase tracking. More precisely the tracking of the carrier-phase as measured at the reference point on the receiver's platform. For the setup used in the simulation studies, shown in Fig. 8 the first antenna is placed at the origin of the body-frame. Therefore the measured carrier-phase equals the one obtained by a receiver only connected to this antenna.

The comparison of this measured carrier-phase with the true one is shown in Fig. 10. It can be seen that only a few seconds are needed until a robust lock is achieved.

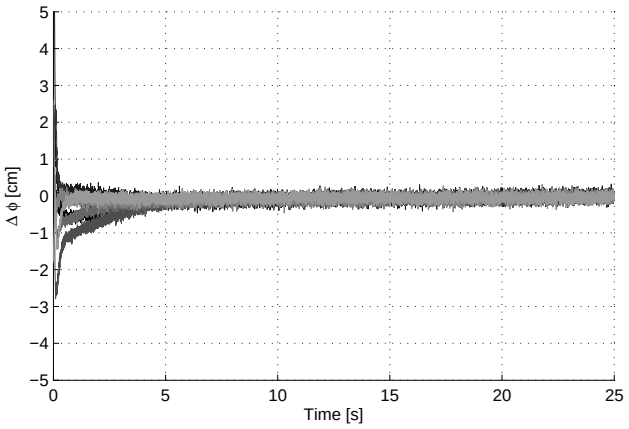

Fig. 10. Carrier-phase measurement error for the first antenna.

8.3 Positioning

It was shown in [9] that in a multisatellite tracking loop with position estimation, the inclusion of the carrier-phase results in a sort of position smoothing. Since in the simulation four antennas were considered, the smoothing has a large time-constant and therefore needs much time to settle. This is illustrated in Fig. 11. It takes some 15 seconds until the position estimation converged to the true one.

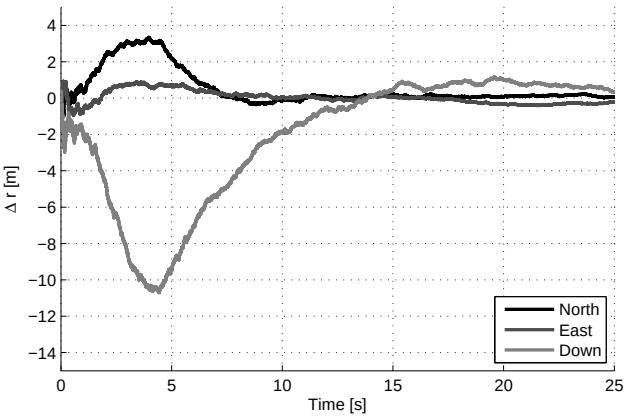

Fig. 11. Positioning Error.

9 CONCLUSION

The analysis of the carrier-phases of the satellite signals measured by multiple antennas shows that the phases can be split up into three parts: a satellite-specific part (the same for all antennas), an antenna-satellite specific part, and an antenna bias. Those three parts can directly be related to the carrier-phase discriminator measurements. Specific attention is drawn to the second part as it contains information about the receiver platform orientation, or attitude. It can be concluded that when the signals from the

antennas are combined after correlation and discrimination – in contrast to digital beamforming, where the antenna signals are directly combined after A/D conversion – the attitude of the platform can be estimated inside the tracking loop. The drawback of this approach, as compared to digital beamforming, is the reduced ability to suppress interference and enhance satellite signals. But still a large gain is achieved by exploiting the spatial correlation among the received satellite signals in a coherent multisatellite tracking loop.

ACKNOWLEDGEMENTS

The authors would like to thank the German Federal Ministry of Economic Affairs and Technology (BMWi) and the German Aerospace Center (DLR) for a financial grant (FKZ: 50NA0911).

REFERENCES

[1] C. J. Hegarty, D. Bobyn, J. Grabowski, and A. J. Van Dierendonck, "An overview of the effects of out-of-band interference on GNSS receivers," in *Proc. ION GNSS*, Sept. 2011.

[2] P. Capozza, B. Holland, T. Hopkinson, and R. Landrau, "A single-chip narrow-band frequency-domain excisor for a global positioning system (GPS) receiver," *IEEE Journal of Solid-State Circuits*, vol. 35, pp. 401–411, Mar. 2000.

[3] P. D. Groves, *Principles of GNSS, Inertial, and Multisensor Integrated Navigation Systems*. Artech House, Inc., 2007.

[4] J. J. Spilker Jr., "Fundamentals of signal tracking theory," in *Global Positioning System: Theory and Applications* (B. W. Parkinson and J. J. Spilker Jr., eds.), vol. 1, pp. 245–327, AIAA, Inc., 1996.

[5] M. Cuntz, M. Heckler, S. Erker, A. Konovaltsev, M. Sgammini, A. Hornbostel, A. Dreher, and M. Meurer, "Navigating in the Galileo test environment with the first GPS/Galileo multi-antenna-receiver," in *Proc. 5th ESA Workshop on Satellite Navigation Technologies (NAVITEC)*, Dec. 2010.

[6] M. L. Psiaki and H. Jung, "Extended Kalman filter methods for tracking weak GPS signals," in *Proc. International Technical Meeting, Institute of Navigation ION*, pp. 2539–2553, Sept. 2002.

[7] H. L. Van Trees, *Optimum array processing*, vol. 4 of *Detection, estimation and modulation theory*. Wiley-Interscience, 2002.

[8] K. Giger, P. Henkel, and C. Günther, "Multifrequency multisatellite carrier tracking," in *Proc. Fourth European Workshop on GNSS Signals and Signal Processing*, Dec. 2009.

[9] K. Giger and C. Günther, "Position domain joint tracking," in *Proc. 5th ESA Workshop on Satellite Navigation Technologies (NAVITEC)*, Dec. 2010.

[10] R. G. Brown and P. Y. C. Hwang, *Introduction to Random Signals and Applied Kalman Filtering*. John Wiley & Sons, Inc., 1992.

[11] M. D. Shuster, "Survey of attitude representations," *Journal of the Astronautical Sciences*, vol. 41, pp. 439–517, Oct. 1993.

[12] F. Landis Markley, "Attitude error representations for Kalman filtering," *Journal of Guidance, Control, and Dynamics*, vol. 26, no. 2, pp. 311–317, 2003.

[13] E. J. Lefferts, L. F. Markley, and M. D. Shuster, "Kalman filtering for attitude estimation," *Journal of Guidance, Control, and Dynamics*, vol. 5, no. 5, pp. 417–429, 1982.

[14] D. Titterton and J. Weston, *Strapdown Inertial Navigation Technology*. Institution of Electrial Engineers (IEE), second ed., 2004.

[15] J. Wendel, *Integrierte Navigationssysteme – Sensordatenfusion, GPS und Inertiale Navigation*. Oldenbourg Wissenschaftsverlag GmbH, 2007.

[16] K. Nipp and D. Stoffer, *Lineare Algebra*. vdf Hochschulverlag AG, fourth ed., 1998.

[17] M. Gómez Arias, "Adaptive Kalman filter-based phase-tracking in GNSS," master thesis, Technische Universität München, Munich, Germany, 2010.

[18] R. Mehra, "Approaches to adaptive filtering," *IEEE Transactions on Automatic Control*, vol. 17, pp. 693–698, Oct. 1972.

[19] J. Betz and K. Kolodziejski, "Generalized theory of code tracking with an early-late discriminator part I: Lower bound and coherent processing," *IEEE Transactions on Aerospace and Electronic Systems*, vol. 45, pp. 1538–1556, October 2009.

[20] K. Giger and C. Günther, "Multisatellite tracking GNSS receivers in multipath environments," in *Proc. ION GNSS*, Sept. 2011.